

Strain-optic coefficients of individual cladding modes of singlemode fibre: theory and experiment

C. Chen and J. Albert

The different strain-optic coefficients for the effective indices of the core and cladding modes of a standard telecom singlemode fibre are measured by stretching a fibre in which a 4°-tilted fibre Bragg grating has been written. The origin of the modal dependence of the strain-optic coefficient differences is analysed and discussed. Good agreement between theoretical and experimental values of these coefficients is reported.

Introduction: Fibre Bragg gratings (FBGs) are widely used as sensors of pressure-strain, temperature, microbending and external refractive index [1–4]. These optical sensors are inherently immune from electromagnetic interference, chemically inert, and they are very attractive in biochemical applications and hazardous surroundings. In conventional FBGs, the Bragg wavelength shift of the guided core mode is determined solely by strain and temperature, therefore with a single wavelength shift measurement it is impossible to distinguish these two factors in one FBG. To simultaneously measure strain and temperature, it is necessary to use two FBGs, a hybrid FBG with long period gratings (LPGs), superimposed FBGs and high birefringence fibre gratings, which increase the complexity of the sensors.

Weakly tilted fibre Bragg gratings (TFBGs) [5, 6] with grating planes tilted at small angles ($\theta < 5^\circ$) relative to the fibre axis couple light both to backward propagating core modes (LP₀₁) and cladding modes (lm) [7]. It has been demonstrated experimentally that the resonant wavelengths for these mode couplings depend differentially on external perturbations [6]. In this Letter we report the first analysis of the differential strain-optic coefficients for the cladding modes in weakly TFBGs and we present strong supporting experimental evidence for our analysis.

Analysis: As is well known, the Bragg reflection and cladding mode resonance wavelengths λ_B and λ_{clad}^i of TFBGs are determined by a phase-matching condition and can be expressed as follows [6]:

$$\lambda_B = 2n_{eff}\Lambda / \cos\theta \quad (1)$$

$$\lambda_{clad}^i = (n_{eff}^i + n_{clad}^i)\Lambda / \cos\theta \quad (2)$$

where n_{eff} , n_{eff}^i and n_{clad}^i are the effective indices of the core mode at λ_B and the core mode and the i th cladding mode at λ_{clad}^i , respectively, and Λ and θ are the period and the internal tilt angle of the TFBG. The wavelength shifts $\Delta\lambda_B$ and $\Delta\lambda_{clad}^i$ caused by longitudinal strain changes ($\Delta\varepsilon$) can be written as follows [8]:

$$\Delta\lambda_B = \lambda_B(1 - p_B)\Delta\varepsilon \quad (3)$$

$$\Delta\lambda_{clad}^i = \lambda_{clad}^i(1 - p_{clad}^i)\Delta\varepsilon \quad (4)$$

where $p_B = -(1/n_{eff})(\partial n_{eff}/\partial\varepsilon)$ and $p_{clad}^i = -1/(n_{eff}^i + n_{clad}^i)(\partial(n_{eff}^i + n_{clad}^i)/\partial\varepsilon)$ are photoelastic coefficients for core (Bragg) mode and the i th cladding modes, respectively, which may be calculated through core and cladding refractive index changes by

$$\delta n = 0.5n^3[p_{12} - \nu(p_{11} - p_{12})]\delta\varepsilon \quad (5)$$

where p_{11} and p_{12} represent the component of the strain-optic tensor, ν is the Poisson ratio and n is the core or cladding refractive index. The high-order cladding modes have smaller effective indices and hence will have larger photoelastic coefficients than the core mode if the partial derivatives of all the effective indices with respect to a global strain change on the fibre are similar. From (3) and (4) and noting that $\lambda_B > \lambda_{clad}^i$ and $p_B < p_{clad}^i$ for high-order cladding modes, we obtain:

$$\begin{aligned} \Delta\lambda_B &= \lambda_B(1 - p_B)\Delta\varepsilon > \lambda_{clad}^i(1 - p_B)\Delta\varepsilon \\ &> \lambda_{clad}^i(1 - p_{clad}^i)\Delta\varepsilon = \Delta\lambda_{clad}^i \end{aligned} \quad (6)$$

So the Bragg peak should have a larger wavelength shift than high-order cladding mode resonances.

Results: The TFBG is written in a CORNING SMF 28 fibre using KrF excimer laser light at 248 nm, and a phase mask to generate the

grating pattern in hydrogen-loaded fibres. The internal tilt angle was determined from the external angle by Snell's law. Fig. 1 shows the transmission spectrum and relative wavelength shifts of cladding modes relative to core modes with longitudinal strain for a TFBG with tilted angle $\sim 4.0^\circ$. From Fig. 1, it can be seen that there are three differential wavelength shift regions: (i) the ghost mode region which is close to the Bragg wavelength is formed by several cladding modes combined together, so it is very sensitive to external strain perturbations; (ii) the low wavelength high-order cladding modes region, where there are several cladding modes which appear to have a very large irregular wavelength shift (possibly due to the double peaks in each resonance which come from the splitting of vector modes); (iii) the well behaved, almost linear differential wavelength shift region between the ghost mode region and the low wavelength region.

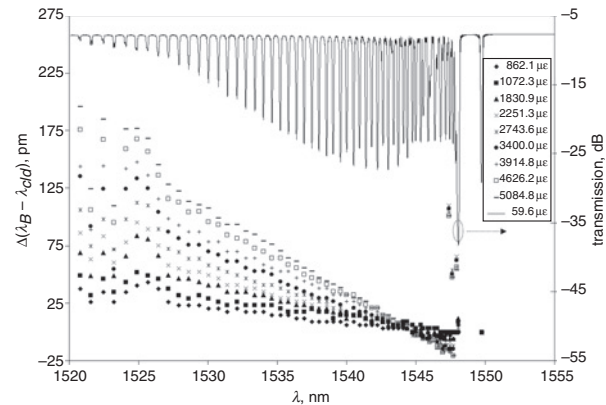


Fig. 1 Transmission spectrum of weakly tilted FBG and differential wavelength shift due to strain changes

For comparison, the temperature sensitivity of the differential wavelength shift of cladding modes relative to the core mode wavelength shift is shown in Fig. 2. The experimental results show that within the temperature range from -9.4 to 69.5°C , the relative cladding mode shifts are less than ± 12 pm or equivalent to $\pm 1.2^\circ\text{C}$ change in over $\sim 80^\circ\text{C}$. Therefore, a temperature insensitive sensor can be made by monitoring the relative core and cladding mode wavelength shifts in the transmission spectrum.

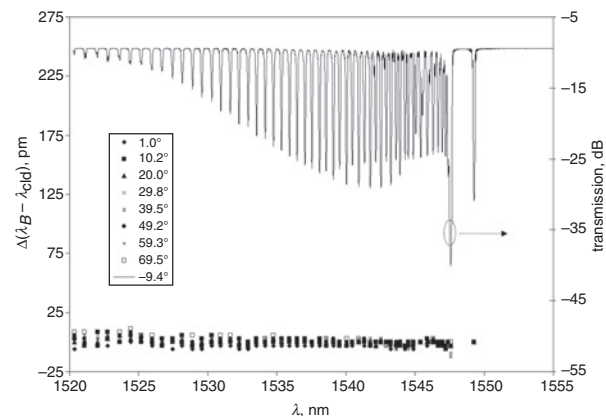


Fig. 2 Transmission spectrum of weakly tilted FBG and differential wavelength shift due to temperature changes

Fig. 3 shows the experimental and analytical results for the differential wavelength shift of mode LP₁₂₆ which has a resonance wavelength ~ 1530 nm relative to the LP₀₁ resonance against strain. The error bars on the experimental result reflect the maximum temperature error $\sim \pm 6$ pm for $\sim 80^\circ\text{C}$ temperature change that is observed in the wavelength shift region that shows regular behaviour (region (iii) above). The analytical result is obtained by (3) and (4), where the partial derivatives of all the effective indices with respect to strain have been replaced by the value for bulk silica, obtained from (5) with $p_{11} = 0.121$ and $p_{12} = 0.27$, and Poisson ratio $\nu = 0.17$ [9]. It can be seen that even with this approximation, the analytical and experimental results are in a good agreement (the small remaining difference reflecting the effect of

the dopant materials and waveguide dispersion on the partial derivatives making up (3) and (4).

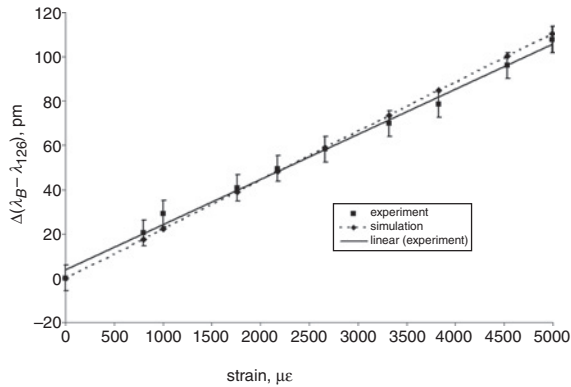


Fig. 3 Relative wavelength shift of LP_{126} mode to LP_{01} mode for different strains with maximum temperature error

Conclusion: We have shown that the strain sensitivity of cladding mode resonances is markedly different from that of the single core mode and that the difference is explained mostly by the value of the effective index of the mode at the resonance wavelength. Therefore the individual resonances of a weakly TFBG will have larger differential sensitivities than the resonances of multi-FBG or superimposed FBG at different wavelengths since the effective indices of cladding modes are much lower than those of core modes at the same wavelength. Our experimental results confirm this analysis and we find that the strain sensitivity of each cladding mode resonance is well approximated by $p_{clad}^i = -2 / (n_{eff}^i + n_{clad}^i) (\partial(n_{silica}) / \partial \epsilon)$. By monitoring the differential shifts of cladding modes relative to the core mode, and noting that all modes have similar temperature sensitivities, weakly TFBGs are attractive candidates for accurate temperature-independent strain sensors.

Acknowledgments: This work is supported by LxSix Photonics, OGSST, and the Center for Photonic Fabrication Research. J. Albert

is the holder of the Canada Research Chair in Advanced Photonic Components at Carleton University.

© The Institution of Engineering and Technology 2006

25 May 2006

Electronics Letters online no: 20061631

doi: 10.1049/el:20061631

C. Chen and J. Albert (Department of Electronics, Carleton University, 1125 Colonel By Drive, Ottawa, Canada, K1S 5B6)

E-mail: jalbert@doe.carleton.ca

References

- Sheng, H., Fu, M., Chen, T., Liu, W., and Bor, S.: 'A lateral pressure sensor using a fibre Bragg grating', *IEEE Photonics Technol. Lett.*, 2004, **16**, pp. 1146–1148
- Shu, X., Lin, Y., Zhao, D., Gwandu, B., Floreani, F., Zhang, L., and Bennion, I.: 'Dependence of temperature and strain coefficients on fibre grating type and its application to simultaneous temperature and strain measurement', *Opt. Lett.*, 2002, **27**, pp. 701–703
- Baek, S., Jeong, Y., and Lee, B.: 'Characteristics of short-period blazed fiber Bragg gratings for use as macro-bending sensors', *Appl. Opt.*, 2002, **41**, pp. 631–636
- Iadicco, A., Cusano, A., Cutolo, A., Berini, R., and Giordano, M.: 'Thinned fiber Bragg gratings as high sensitivity refractive index sensor', *IEEE Photonics Technol. Lett.*, 2004, **16**, pp. 1149–1151
- Laffont, G., and Ferdinand, P.: 'Tilted short-period fibre-Bragg-grating-induced coupling to cladding modes for accurate refractometer', *Meas. Sci. Technol.*, 2001, **12**, pp. 765–770
- Chen, C., Xiong, L., Jafari, A., and Albert, J.: 'Differential sensitivity characteristics of tilted fibre Bragg grating sensors'. Optics East 2005, *Proc SPIE*, 2005, Paper 6004-13
- Lee, K.S., and Erdogan, T.: 'Fiber mode coupling in transmissive and reflective tilted fibre gratings', *Appl. Opt.*, 2000, **39**, pp. 1394–1404
- Othonos, A., and Kalli, K.: 'Fiber Bragg gratings' (Artech House, Boston, MA, 1999)
- Bertholds, A., and Dandliker, R.: 'High-resolution photoelastic pressure sensor using low-birefringence fiber', *Appl. Opt.*, 1986, **25**, pp. 340–343